Available online at www.sciencedirect.com
ScienceDirect
Trans. Nonferrous Met. Soc. China 23(2013) 3658−3667
Transactions of Nonferrous Metals Society of China
www.tnmsc.cn

Effect of solution treatment and aging on microstructural evolution and mechanical behavior of NiTi shape memory alloy

Shu-yong JIANG[1], Ya-nan ZHAO[1], Yan-qiu ZHANG[1], Li HU[2], Yu-long LIANG[2]

1. Industrial Training Centre, Harbin Engineering University, Harbin 150001, China;
2. College of Materials Science and Chemical Engineering, Harbin Engineering University, Harbin 150001, China

Received 11 January 2013; accepted 9 July 2013

Abstract: As-received nickel−titanium (NiTi) shape memory alloy with a nominal composition of $Ni_{50.9}Ti_{49.1}$ (mole fraction, %) was subjected to solution treatment at 1123 K for 2 h and subsequent aging for 2 h at 573 K, 723 K and 873 K, respectively. The influence of solution treatment and aging on microstructural evolution and mechanical behavior of NiTi alloy was systematically investigated by transmission electron microscopy (TEM), high resolution transmission electron microscopy (HRTEM), scanning electron microscopy (SEM) and compression test. Solution treatment contributes to eliminating the Ti_2Ni phase in the as-received NiTi sample, in which the TiC phase is unable to be removed. Solution treatment leads to ordered domain of atomic arrangement in NiTi alloy. In all the aged NiTi samples, the Ni_4Ti_3 precipitates, the *R* phase and the *B*2 austenite coexist in the NiTi matrix at room temperature, while the martensitic twins can be observed in the NiTi samples aged at 873 K. In the NiTi samples aged at 573 and 723 K, the fine and dense Ni_4Ti_3 precipitates distribute uniformly in the NiTi matrix, and thus they are coherent with the *B*2 matrix. However, in the NiTi sample aged at 873 K, the Ni_4Ti_3 precipitates exhibit the very inhomogeneous size, and they are coherent, semi-coherent and incoherent with the *B*2 matrix. In the case of aging at 723 K, the NiTi sample exhibits the maximum yield strength, where the fine and homogeneous Ni_4Ti_3 precipitates act as the effective obstacles against the dislocation motion, which results in the maximum critical resolved shear stress for dislocation slip.

Key words: NiTi alloy; shape memory alloy; microstructural evolution; mechanical properties; solution treatment; aging

1 Introduction

The remarkable attractiveness of nickel−titanium shape memory alloy (NiTi SMA) comes from its shape memory effect as well as superelasticity. Shape memory effect of NiTi SMA refers to its ability to remember the shape at a certain state. Specifically, NiTi SMA is imparted to a certain shape at the *B*2 austenite phase and then is transformed into the *B*19' martensite phase, where NiTi SMA undergoes a certain plastic deformation at the martensite phase and then is able to go back to the previous shape at the austenite phase on heating. Superelasticity of NiTi SMA refers to its ability to recover its original shape along with the release of stress after NiTi SMA has been deformed beyond its elastic limit by external mechanical stress. The perfect shape memory effect and the superior superelasticity are essential for the engineering application of NiTi SMA [1]. However, chemical composition, heat treatment and plastic working history of NiTi SMA play a significant role in its shape memory effect as well as superelasticity [2−6]. In particular, solution treatment and aging are of great importance in improving the functional properties and the mechanical properties of NiTi SMA. In general, the Ni_4Ti_3 precipitates can arise in the Ni-rich NiTi samples aged at a certain temperature. It is well known that as a metastable phase, the Ni_4Ti_3 precipitate belongs to *R*3 space group and it possesses a rhombohedral unit cell structure [7, 8]. The electron diffraction patterns of the Ni_4Ti_3 precipitate reveal that the diffraction spots are located at 1/7 positions along ⟨321⟩ reciprocal vectors of *B*2 austenite matrix [9,10]. The Ni_4Ti_3 precipitate has an important influence on microstructural evolution and transformation behavior of NiTi SMA. It is generally accepted that the presence of Ni_4Ti_3 precipitates is responsible for the occurrence of *R* phase, which plays a predominant role in multi-stage martensitic

Foundation item: Project (51071056) supported by the National Natural Science Foundation of China; Projects (HEUCF121712, HEUCF201317002) supported by the Fundamental Research Funds for the Central Universities of China
Corresponding author: Shu-yong JIANG; Tel: +86-451-82519706; E-mail: jiangshy@sina.com
DOI: 10.1016/S1003-6326(13)62914-3

transformation of NiTi SMA, where the two-stage phase transformation or the three-stage phase transformation can occur [11−13]. In addition, it is of great importance to investigate the size and distribution of the Ni_4Ti_3 precipitates in the microstructure of NiTi matrix. In general, the size and distribution of the Ni_4Ti_3 precipitates depend on the aging temperature, the aging time, the external stress, the chemical composition and so on. It is well known that the size of the Ni_4Ti_3 precipitates increases with the increase of aging temperature and aging time. It has been reported that the small Ni_4Ti_3 particles less than 100 nm are coherent with the *B*2 austenite matrix, while the Ni_4Ti_3 precipitates shall gradually lose coherency with the increase of size [14−16]. As compared to the stress-free aging, the stress-assisted aging results in the microstructures with a homogeneous distribution of Ni_4Ti_3 precipitates in terms of number density [17]. The homogeneous distribution of the Ni_4Ti_3 precipitates across the whole microstructure occurs more easily in the aged NiTi samples with high Ni content than in those with low Ni content, where the grain boundary plays a predominant role [18−20]. In addition to the transformation behavior, the Ni_4Ti_3 precipitates have an important effect on the mechanical properties and the shape memory behavior of NiTi SMA. It has been reported that in the case of aging at the low temperature, the dense and fine Ni_4Ti_3 precipitates with the size of about 10 nm can substantially increase the critical stress for slip deformation, which contributes to enhancing the hardness and yield strength of NiTi SMA [15,21]. The small Ni_4Ti_3 precipitates which are coherent with the NiTi matrix are capable of improving the fatigue resistance of the NiTi SMA [16]. SHAKERI et al [22] found that the orientation of the Ni_4Ti_3 precipitates has an important influence on the two-way shape memory effect of NiTi SMA and the aging at 723 K for up to 2.5 h contributes to enhancing the recovery ratio.

In the present study, the influence of solution treatment and aging on microstructural evolution and mechanical behavior of NiTi SMA is investigated, where the size and distribution of the Ni_4Ti_3 precipitates are characterized, which lays the sound foundation for understanding the functional properties and mechanical properties of NiTi SMA.

2 Experimental

The as-received NiTi SMA with a nominal composition of $Ni_{50.9}Ti_{49.1}$ (mole fraction, %) was prepared by means of vacuum induction melting method, and then was rolled at 1073 K, and finally was drawn to the NiTi bar with the diameter of 12 mm at 673 K. The NiTi samples with the diameter of 4 mm and height of 6 mm were cut from the NiTi bar by means of electro-discharge machining (EDM). The NiTi samples were subjected to a solution treatment, where the NiTi samples were held for 2 h at 1123 K and then were quenched into ice water. The solution-treated NiTi samples were aged for 2 h at 573, 723 and 873 K, respectively, followed by cooling to room temperature at atmosphere. The heat treatment for all the NiTi samples was carried out in the argon atmosphere. Microstructural evolution of NiTi alloy was investigated by means of transmission electron microscopy (TEM). Foils for TEM observation were mechanically ground to 70 μm and then thinned by twin-jet polishing in an electrolyte consisting of 6% $HClO_4$, 34% $C_4H_{10}O$ and 60% CH_3OH (volume fraction). TEM observations were conducted on a FEI TECNAI G2 F30 microscope with a side-entry and double-tilt specimen stage with angular ranges of ±40° at an accelerating voltage of 300 kV. High resolution transmission electron microscopy (HRTEM) was also conducted in order to investigate the atomic structure of the NiTi sample subjected to solution treatment and aging. The as-received, solution-treated and aged NiTi samples were compressed on INSTRON-5500R at the strain rate of 0.05 s^{-1} at room temperature in order to investigate the mechanical behavior of the corresponding NiTi samples. The fracture photograph of the compressed NiTi samples was observed by means of scanning electron microscopy (SEM) on a FEI Quanta200 microscope.

3 Results and discussion

3.1 Microstructural evolution

3.1.1 Microstructure of as-received NiTi sample

Figure 1 shows TEM photographs and the selected area electron diffraction (SAED) pattern of as-received NiTi alloy. It is clear that the as-received NiTi alloy consists of a *B*2 austenite matrix and an extremely small amount of Ti_2Ni phase and TiC phase. Furthermore, it can be seen from Fig. 1(f) that the as-received NiTi alloy contains plenty of dislocations, which stem from the processing of the NiTi bar. In general, Ti_2Ni phase frequently arises in the Ti-rich NiTi alloy. However, in the present study, Ti_2Ni particles occur in the Ni-rich NiTi alloy, which is probably due to the fact that oxygen leads to the stabilization of Ti_2Ni particles [2]. Carbon is introduced as an impurity and carbon atoms do not dissolve in NiTi solid. Consequently, C reacts with Ti to form TiC. In the present study, it is very difficult to accurately determine the volume fraction of Ti_2Ni and TiC particles, which is out of the scope of the work. However, it can not be denied that the presence of Ti_2Ni and TiC particles leads to the decrease of Ti concentration in the NiTi matrix, which shall be investigated in the future.

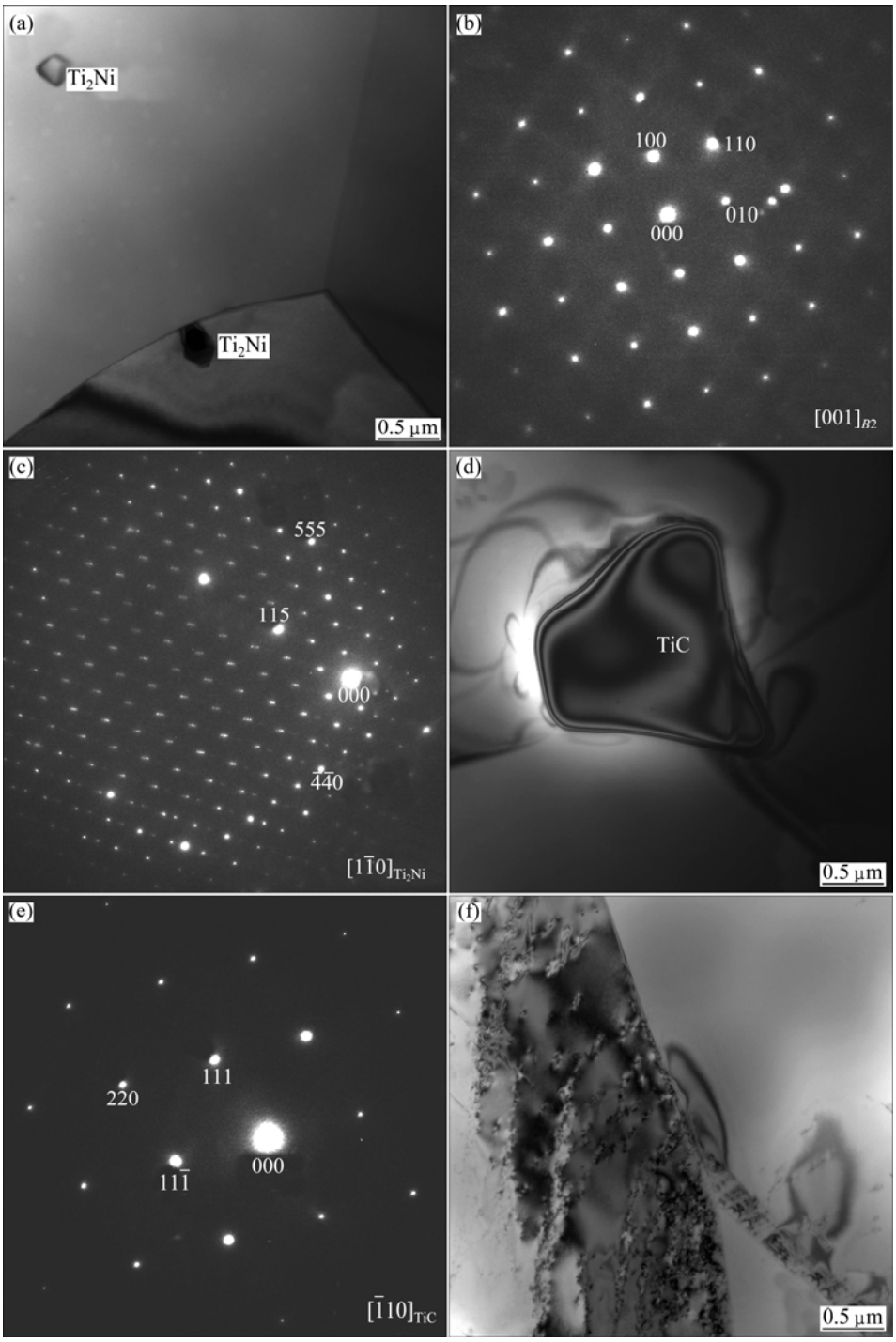

Fig. 1 TEM images of as-received NiTi sample: (a) Image of matrix with Ti_2Ni phase; (b) SAED pattern of matrix showing *B*2 austenite structure; (c) SAED pattern of Ti_2Ni; (d) Image of matrix with TiC phase; (e) SAED pattern of TiC; (f) Matrix with dislocations

3.1.2 Microstructure of solution-treated NiTi sample

Figure 2 illustrates TEM photographs and SAED patterns of solution-treated NiTi specimen. It can be observed from Fig. 2 that after NiTi sample is subjected to solution treatment, the matrix still belongs to *B*2 austenite and TiC phase still exists on the matrix of *B*2 austenite, but Ti_2Ni phase disappears. Therefore, Ti_2Ni phase can be dissolved in the NiTi sample undergoing solution treatment, but TiC particles are unable to be removed from NiTi sample in the case of solution treatment since TiC particles possess very high thermal stability. In addition, solution treatment of NiTi sample at 1123 K for 2 h is capable of making dislocation defects eliminated completely.

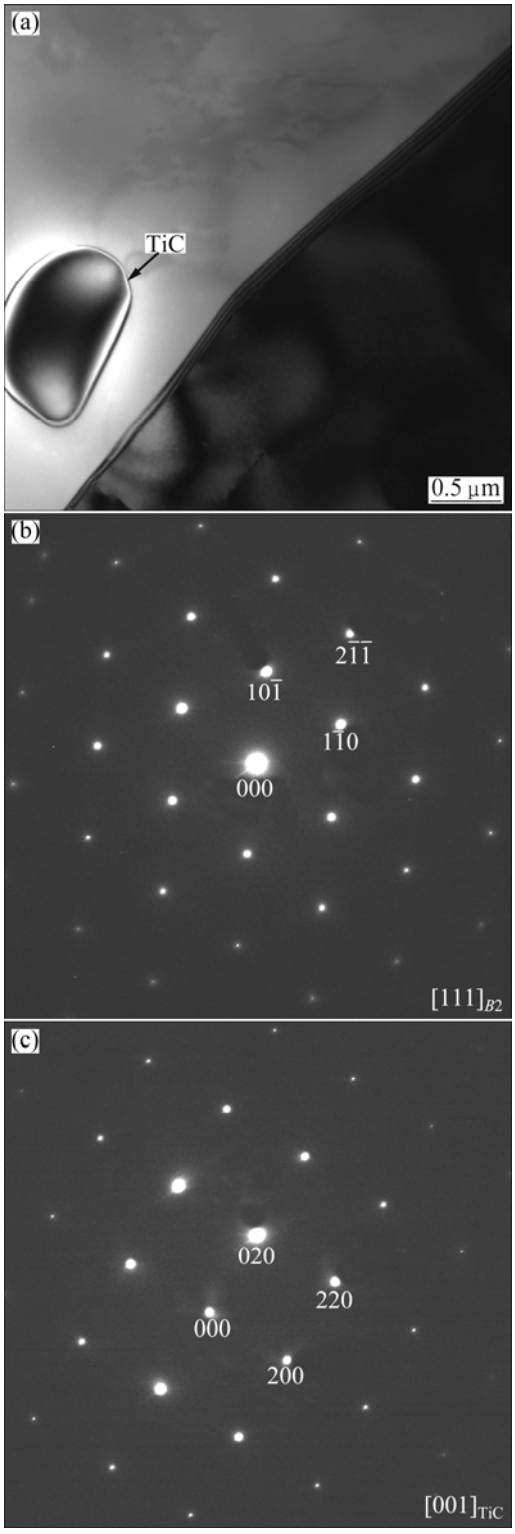

Fig. 2 TEM images of solution-treated NiTi sample: (a) Photograph of matrix; (b) SAED pattern of matrix showing *B*2 austenite structure; (c) SAED pattern of TiC

Figure 3 indicates HRTEM image of solution treated NiTi specimen and the corresponding fast Fourier transform (FFT). It can be seen from FFT in Fig. 3 that the atomic arrangement is characterized by woven pattern, which indicates that the ordered domain occurs

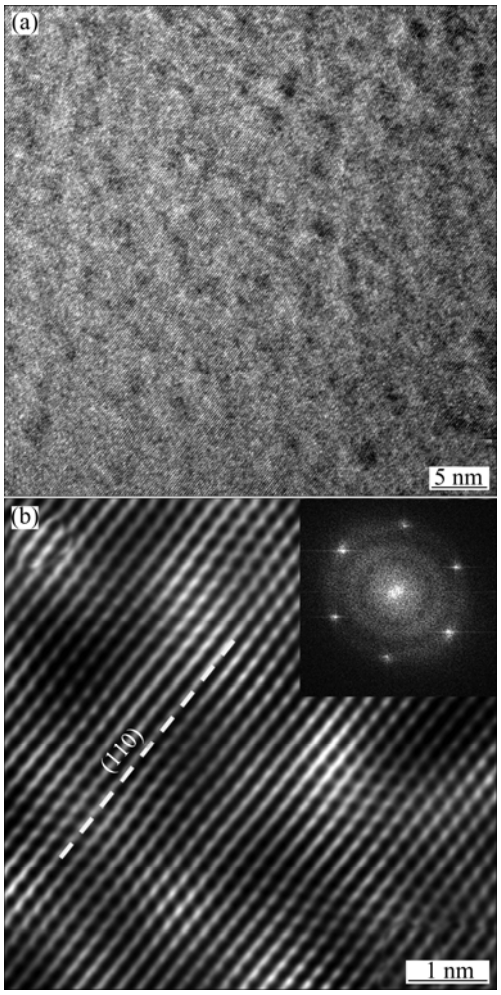

Fig. 3 HRTEM images of solution treated NiTi sample: (a) HRTEM image; (b) FFT image

in the NiTi matrix subjected to solution treatment. According to the phase diagram of binary NiTi alloy, as for NiTi alloy with a Ni-rich composition of $Ni_{50.9}Ti_{49.1}$ (mole fraction, %), the NiTi phase belongs to a single phase zone with a complete solubility at 1123 K [1]. Furthermore, the solubility limit decreases greatly with the decrease in the temperature on the Ni-rich side. When the NiTi samples are held for 2 h at 1123 K and then followed by quenching in ice water, supersaturated solid solution occurs so that the Ni atoms are unable to uniformly distribute in the NiTi matrix. The Ni atoms shall be partially accumulated on the (110) plane, which leads to the occurrence of the short-range order structure in the NiTi matrix.

3.1.3 Microstructure of aged NiTi samples

Figures 4−6 indicate TEM photographs of the NiTi samples aged at 573, 723 and 873 K, respectively. In the NiTi samples aged at 573 K and 723 K, the fine Ni_4Ti_3 precipitate phases are homogeneously dispersed in the NiTi matrix, while the Ni_4Ti_3 precipitates exhibit the inhomogeneous distribution in the matrix of NiTi sample

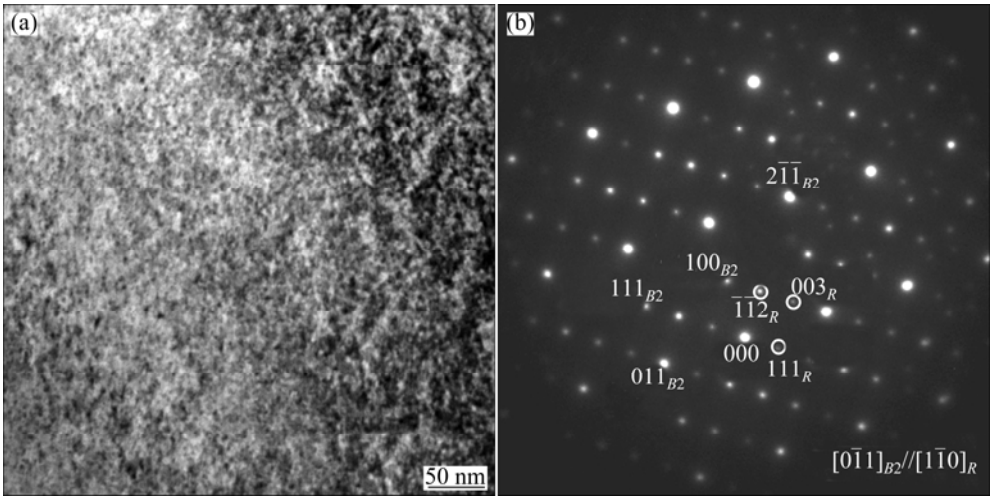

Fig. 4 TEM images of NiTi sample aged at 573 K: (a) Bright field image; (b) SAED pattern of (a) showing orientation relationship between *R* phase and *B*2 austenite matrix

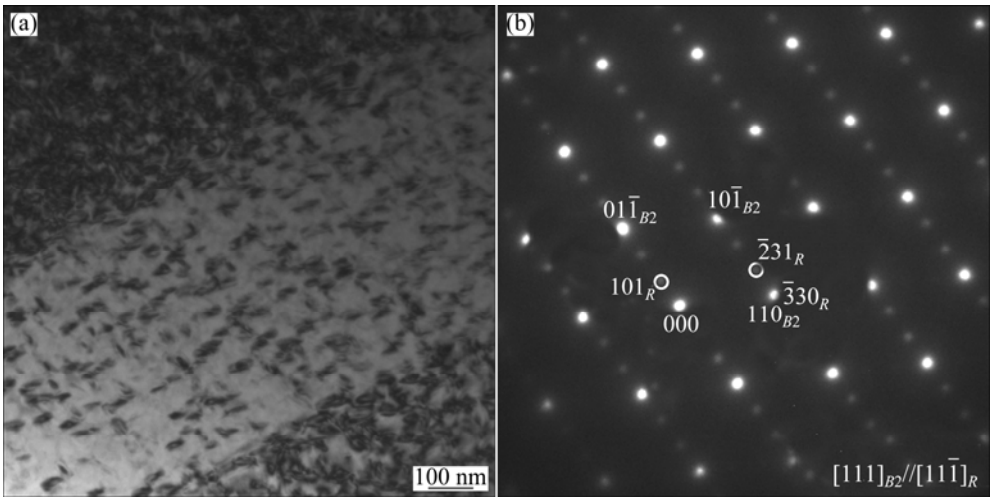

Fig. 5 TEM images of NiTi sample aged at 723 K: (a) Bright field image; (b) SAED pattern of (a) showing orientation relationship between *R* phase and *B*2 austenite matrix

aged at 873 K. Furthermore, it can be found from Fig. 6 that the Ni_4Ti_3 precipitates are relatively coarser in the grain interior than in the grain boundary, and they are characterized by the typical lenticular shape. It can be observed by means of the corresponding SAED pattern that in the NiTi samples aged at 573, 723 and 873 K, the Ni_4Ti_3 precipitates, the *R* phase and the *B*2 austenite coexist in the NiTi matrix at room temperature. In addition, in the NiTi samples aged at 873 K, the martensitic twins are observed and thus the martensitic transformation occurs.

The size of the Ni_4Ti_3 precipitates was estimated by means of TEM images, in which the diameter of the Ni_4Ti_3 precipitates can be obtained by combining DigitalMicrograph software with equal perimeter method. It can be found that the size of the Ni_4Ti_3 precipitates increases with the increase of the aging temperature. In the NiTi sample aged at 573 K, the Ni_4Ti_3 precipitates show the uniform size, where the average size of the Ni_4Ti_3 precipitates is about 5 nm. In the NiTi sample aged at 723 K, the Ni_4Ti_3 precipitates also show the uniform size, where the average size of the Ni_4Ti_3 precipitates is about 50 nm. However, in the NiTi sample aged at 873 K, the Ni_4Ti_3 precipitates exhibit the very inhomogeneous size, where the average size of the Ni_4Ti_3 precipitates is about 200 nm, while the maximum precipitation size is about 1200 nm, and the minimum precipitation size is about 40 nm. It is necessary to investigate the size of the Ni_4Ti_3 precipitates since whether the Ni_4Ti_3 phase is coherent with the *B*2 matrix or not depends on the size of the Ni_4Ti_3 precipitates. It has been reported that the fine Ni_4Ti_3 precipitate is coherent with the *B*2 matrix in the Ni-rich NiTi sample aged at 723 K for 3 h, where the size of the Ni_4Ti_3 precipitate is approximately 60 nm [14]. However, in the Ni-rich NiTi sample aged at 873 K for 20 h, the large

Ni_4Ti_3 precipitate possesses a semi-coherent interface with the *B*2 matrix, where the size of the Ni_4Ti_3 precipitate is not measured [14]. GALL et al [15,16] found that the Ni_4Ti_3 precipitates up to approximately 100 nm in size remain coherent with the *B*2 matrix, while the Ni_4Ti_3 precipitates with 500 nm lose coherency with the *B*2 matrix completely. In our study, it can be inferred that the Ni_4Ti_3 precipitates keep the coherent interface with the *B*2 matrix in the NiTi sample aged at 573 and 723 K, while the Ni_4Ti_3 precipitates which are coherent, semi-coherent and incoherent with the *B*2 matrix coexist in the NiTi sample aged at 873 K. Figure 7 shows

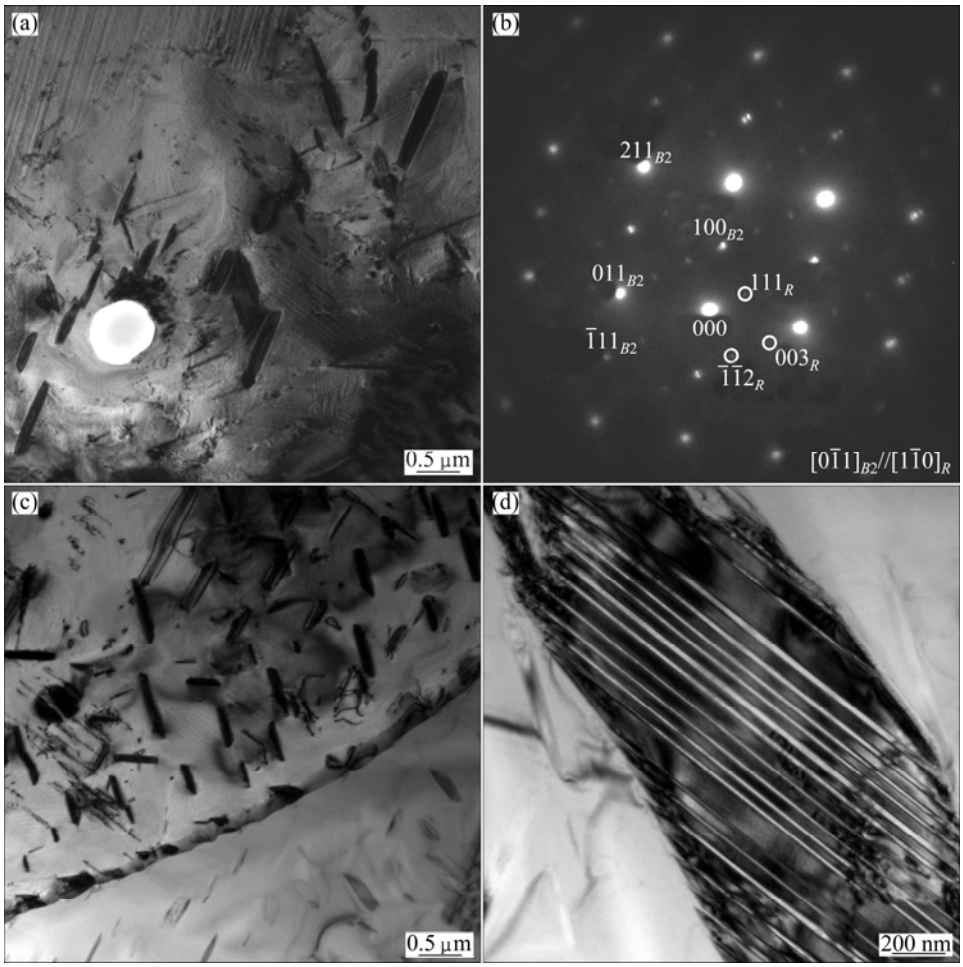

Fig. 6 TEM images of NiTi sample aged at 873 K: (a) Precipitation of Ni_4Ti_3 in grain interior; (b) SAED pattern of matrix showing orientation relationship between *R* phase and *B*2 austenite matrix; (c) Precipitation of Ni_4Ti_3 in grain boundary; (d) Martensitic twins

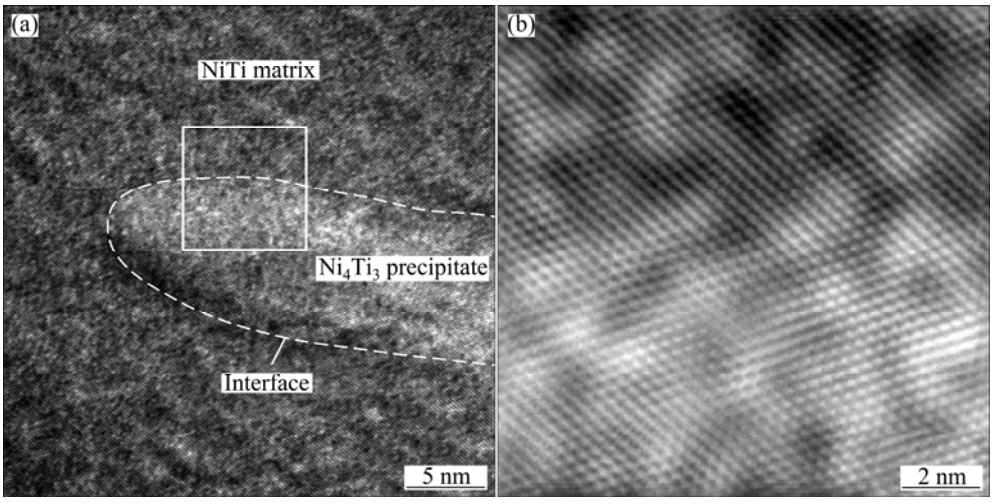

Fig. 7 HRTEM image of NiTi sample aged at 723 K: (a) Interface between Ni_4Ti_3 precipitate and NiTi matrix; (b) FFT of square area in (a) showing coherent relationship between Ni_4Ti_3 precipitate and NiTi matrix

HRTEM image of the NiTi sample aged at 723 K and the corresponding FFT. It can be seen from Fig. 7 that the Ni_4Ti_3 precipitate keeps the completely coherent relationship with the NiTi matrix.

The size of Ni_4Ti_3 precipitates has an important influence on the phase transformation of the NiTi alloy. When the Ni_4Ti_3 precipitate is coherent with the *B*2 austenite matrix, the *R* phase nucleates more easily at the interface between the Ni_4Ti_3 precipitate and the *B*2 austenite matrix in order to relax the coherent stress. However, when the Ni_4Ti_3 precipitate is incoherent with the *B*2 austenite, the dislocation networks occur at the interface between the Ni_4Ti_3 precipitate and the *B*2 austenite matrix, which probably suppresses the formation of the *R* phase and thus leads to the occurrence of the martensitic transformation. The small-scale chemical composition inhomogeneity in the *B*2 austenite matrix between the Ni_4Ti_3 precipitates leads to one *B*2−*R* phase transformation and two *R*−*B*19' phase transformations. Furthermore, the two R-B19' transformations occur at low Ni region near the Ni_4Ti_3 precipitate and at high Ni region away from the Ni_4Ti_3 precipitate, respectively [11,12]. The large-scale inhomogeneity between grain boundary region and grain interior region plays a considerable role in the three-stage transformation on cooling, where the first transformation and the second transformation correspond to the transformation from *B*2 austenite to *R*-phase and then the transformation from *R*-phase to *B*19' martensite at the grain boundary regions containing the Ni_4Ti_3 precipitates, respectively, and the third transformation corresponds to the transformation from *B*2 austenite to *B*19' martensite in the grain interior regions which are free of Ni_4Ti_3 precipitates [17]. However, it is generally accepted that the homogeneous distribution of the Ni_4Ti_3 precipitates in the NiTi matrix can result in the two-stage transformation of *B*2−*R*−*B*19', where the *R*-phase first nucleates and grows at the interface between the Ni_4Ti_3 precipitate and the *B*2 austenite matrix, and the *B*19' martensite nucleates and grows at the interface between the Ni_4Ti_3 precipitate and the *R*-phase [20]. In the present study, whether the aged NiTi samples exhibit the muliti-stage phase transformation or not needs to be further investigated by differential scanning calorimetry (DSC) in the future, which is out of the scope of the work and shall be published in another literature.

3.2 Mechanical behavior of NiTi sample under compression

Figure 8 shows the stress−strain curves of the as-received, solution-treated and aged NiTi samples before compressive fracture, respectively. It can be found from Fig. 8 that as compared to the as-received NiTi sample, the NiTi sample aged at 573 and 723 K possesses the higher yield strength and the solution-treated NiTi sample exhibits the lower yield strength. However, the NiTi sample aged at 873 K shows the similar stress−strain curve with the as-received NiTi sample. In addition, it can be seen from Fig. 8 that as compared to the solution-treated NiTi sample, all the aged NiTi samples exhibit higher yield strength. Furthermore, among all the aged NiTi samples, the NiTi sample aged at 723 K possesses the maximum yield strength and the NiTi sample aged at 873 K possesses the minimum yield strength. Figure 9 shows fractographs of the corresponding compressed NiTi samples. It can be found from Fig. 9 that all the fractographs are characterized by a mixture of brittle fracture and ductile fracture, and the ductile fracture features are gradually dominant with the increase of the aged temperature. For instance, it can be obviously seen in the NiTi sample aged at 873 K that the cleavage fracture surface plays a slight role, but the void growth prevails which reveal that the ductile fracture is more dominant.

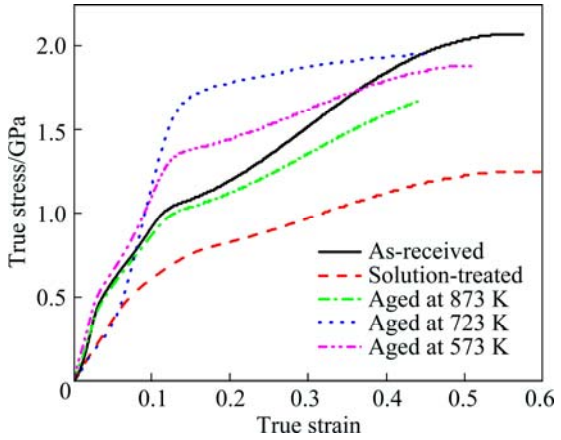

Fig. 8 Stress−strain curves of NiTi samples under compression

According to the above results, it can be found that in the NiTi samples aged at 573, 723 and 873 K, the Ni_4Ti_3 precipitates, the *R* phase and the *B*2 austenite coexist in the NiTi matrix at room temperature. Therefore, the mechanical behavior of the aged NiTi samples under compressive loading is very complicated since the reorientation of the *R* phase, the stress-induced martensite transformation of the *R* phase and the stress-induced martensite transformation of the *B*2 austenite occur probably during compression deformation. To investigate the transformation behavior of the aged NiTi samples under compressive loading is out of the scope of the work. In the present study, the emphasis is laid on the influence of the Ni_4Ti_3 precipitates on the mechanical properties of the NiTi samples. It can be seen from Fig. 8 that the NiTi samples aged at the three temperatures exhibit higher yield strength than those subjected to solution treatment,

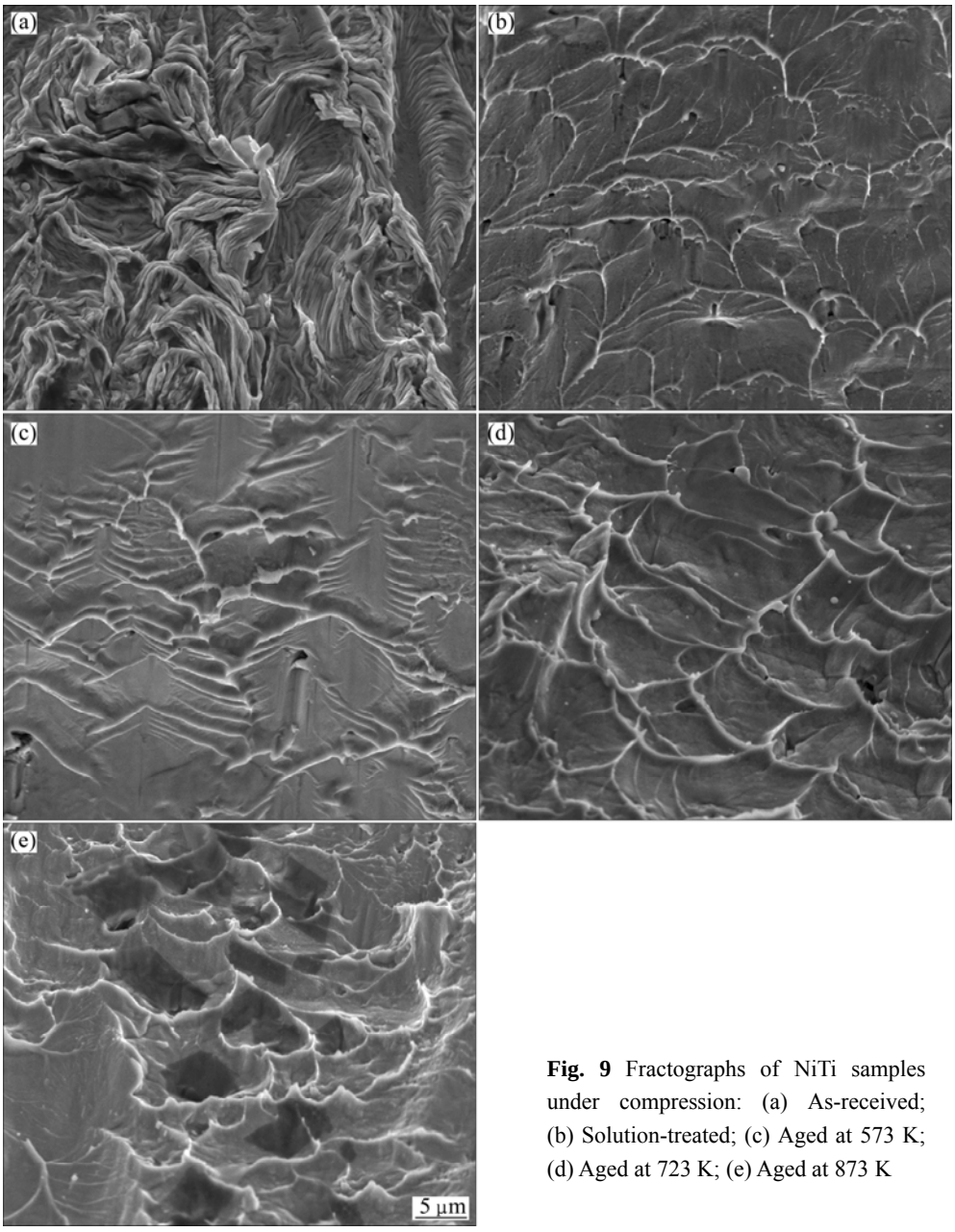

Fig. 9 Fractographs of NiTi samples under compression: (a) As-received; (b) Solution-treated; (c) Aged at 573 K; (d) Aged at 723 K; (e) Aged at 873 K

which indicates that the Ni_4Ti_3 precipitates play an important role in strengthening the NiTi matrix, where the size of the Ni_4Ti_3 precipitates is a crucial factor. It is well known that the physical mechanism of Ni_4Ti_3 precipitates for enhancing the yield strength of the NiTi sample is attributed to the impediment of the Ni_4Ti_3 precipitates to dislocation motion, which leads to the increase of the critical resolved shear stress for dislocation slip. However, it is evident from Fig. 8 that in the case of the three different aging temperatures, the Ni_4Ti_3 precipitates have a different effect on enhancing the yield strength of the NiTi samples, which is closely associated with the size of the Ni_4Ti_3 precipitates. In the NiTi samples aged at 573 K, the fine Ni_4Ti_3 precipitates have only the size of about 5 nm, and they are coherent with the NiTi matrix, but the coherent stress field is very small. It has been reported that in terms of aging at the low temperature, the critical resolved shear stress for dislocation slip possesses the maximum value in the NiTi sample with the Ni_4Ti_3 precipitates of about 10 nm in size [14,21]. Accordingly, the critical resolved shear stress for dislocation slip increases with the increase of the Ni_4Ti_3 precipitate in size when the size of the Ni_4Ti_3 precipitate is less than a critical value. In the NiTi samples aged at 573 K for 2 h, the Ni_4Ti_3 precipitates can not reach the maximum size as well as the maximum density due to the shorter aging time, so the critical resolved shear stress for dislocation slip is unable to reach the maximum value as well. In addition, the oversaturated Ni atoms can not precipitate completely

from the NiTi matrix at the shorter aging time, so the matrix of the NiTi samples aged at 573 K for 2 h remains a certain supersaturated state. It can be found from Figs. 9(c) and (d) that the NiTi sample aged at 573 K exhibits the partially similar fractograph characteristic as that subjected to solution treatment. In the NiTi samples aged at 873 K, the Ni_4Ti_3 precipitates are larger in size, and some of the large precipitates lose coherency with the NiTi matrix. As a result, the dislocation networks arise at the interface between the Ni_4Ti_3 precipitate and the NiTi matrix. The occurrence of the dislocation networks contributes to the plastic deformation of the NiTi sample for dislocation slip. Therefore, on the one hand, the Ni_4Ti_3 precipitates result in the resistance to dislocation movement, which contributes to increasing the critical resolved shear stress for dislocation slip. On the other hand, the existence of the dislocation networks facilitates the plastic deformation for dislocation slip, which leads to decreasing the critical resolved shear stress for dislocation slip. As a consequence, the competition between the above two factors comes to a compromise in terms of strengthening the NiTi matrix. In addition, the inhomogeneous distribution of the Ni_4Ti_3 precipitates in the NiTi matrix has an adverse influence on raising the yield strength of the NiTi sample. However, it can not be denied that as compared to the solution treatment, the aging at 873 K plays a certain role in strengthening the NiTi matrix and enhancing its plasticity, where the fractograph is characterized by a more dominant ductile fracture, as shown in Fig. 9(d). In the NiTi samples aged at 723 K, the adequate precipitation of the Ni atoms in the supersaturated NiTi matrix results in a high density of Ni_4Ti_3 particles, where the distance between the Ni_4Ti_3 precipitates is very small. Therefore, the fine Ni_4Ti_3 precipitates disperse homogeneously in the NiTi matrix, and they keep the perfect coherent interface with the NiTi matrix, where the coherent stress field is very large. The fine and dense Ni_4Ti_3 precipitates act as the effective obstacles against the movement of dislocations, which results in the increase of the critical resolved shear stress for dislocation slip. In addition, the interaction between the coherent stress field and the dislocation stress field leads to the increase of the critical resolved shear stress for dislocation slip. It can be deduced that as compared to the NiTi samples aged at 573 and 873 K, the NiTi samples aged at 723 K exhibit the more comprehensive mechanical properties. In particular, the NiTi samples aged at 723 K shall probably possess the better superelasticity and shape memory effect, which needs to be investigated in the future.

4 Conclusions

1) Solution treatment contributes to eliminating the Ti_2Ni phase in the as-received NiTi sample. However, the TiC phase is unable to be removed by means of solution treatment since TiC particles possess very high thermal stability. Solution treatment leads to ordered domain of atomic arrangement in the NiTi alloy. Furthermore, solution treatment is capable of eliminating the total dislocation defects in the as-received NiTi sample.

2) In all the aged NiTi samples, the Ni_4Ti_3 precipitates, the *R* phase and the *B*2 austenite coexist in the NiTi matrix at room temperature, while the martensitic twins are observed in the NiTi samples aged at 873 K. In the NiTi samples aged at 573 and 723 K, the fine and dense Ni_4Ti_3 precipitates distribute uniformly in the *B*2 matrix, and thus they are coherent with the *B*2 matrix. However, in the NiTi sample aged at 873 K, the Ni_4Ti_3 precipitates exhibit the very inhomogeneous size, and they are coherent, semi-coherent and incoherent with the *B*2 matrix.

3) As compared to the solution treatment, the aging at 723 K leads to the maximum yield strength of NiTi alloy, where the fine and homogeneous Ni_4Ti_3 precipitates are coherent with the NiTi matrix, and thus they act as the effective obstacles against the movement of the dislocations, which results in the increase of the critical resolved shear stress for dislocation slip. However, the aging at 873 K leads to the minimum yield strength of NiTi alloy, where the occurrence of the dislocation networks at the interface between the incoherent Ni_4Ti_3 precipitates and the NiTi matrix contributes to the plastic deformation of the NiTi sample for dislocation slip, which results in the decrease of the critical resolved shear stress for dislocation slip.

References

[1] OTUKA K, REN X. Physical metallurgy of Ti−Ni-based shape memory alloys [J]. Progress in Materials Science, 2005, 50: 511−678.

[2] FRENZEL J, GEORGE E P, DLOUHÝ A, SOMSEN C, WAGNER M F X, EGGELER G. Influence of Ni on martensitic phase transformations in NiTi shape memory alloys [J]. Acta Materialia, 2010, 58(9): 3444−3458.

[3] MITWALLY M E, FARAG M. Effect of cold work and annealing on the structure and characteristics of NiTi alloy [J]. Materials Science and Engineering A, 2009, 519(1−2): 155−166.

[4] HUANG X, LIU Y. Effect of annealing on the transformation behavior and superelasticity of NiTi shape memory alloy [J]. Scripta Materialia, 2001, 45(2): 153−160.

[5] JIANG Shu-yong, ZHANG Yan-qiu. Microstructure evolution and deformation behavior of as-cast NiTi shape memory alloy under compression [J]. Transactions of Nonferrous Metals Society of China, 2012, 22(1): 90−96.

[6] JIANG Shu-yong, ZHANG Yan-qiu. Fracture behavior and microstructure of as-cast NiTi shape memory alloy [J]. Transactions of Nonferrous Metals Society of China, 2012, 22(6): 1401−1406.

[7] SABURI T, NENNO S, FUKUDA T. Crystal structure and morphology of the metastable X phase in shape memory Ti−Ni alloys [J]. Journal of the Less-Common Metals, 1986, 125: 157−166.
[8] TADAKI T, NAKATA Y, SHIMIZU K, OTSUKA K. Crystal structure, composition and morphology of a precipitate in an aged Ti−51at%Ni shape memory alloy [J]. Transactions of the Japan Institute of Metals, 1986, 27(10): 731−740.
[9] NISHIDA M, WAYMAN C M, KAINUMA R, HONMA T. Further electron microscopy studies of the $Ti_{11}Ni_{14}$ phase in an aged Ti−52at.%Ni shape memory alloy [J]. Scripta Metallurgica, 1986, 20: 899−904.
[10] NISHIDA M, WAYMAN C M. Electron microscopy studies of precipitation process in near-equiatomic TiNi shape memory alloys [J]. Materials Science and Engineering, 1987, 93:191−203.
[11] ALLAFI K J, REN X, EGGELER G. The mechanism of multistage martensitic transformations in aged Ni-rich NiTi shape memory alloys [J]. Acta Materialia, 2002, 50(4): 793−803.
[12] KHALIL-ALLAFI J, EGGELER G, DLOUHY A, SCHMAHL W W, SOMSEN C. On the influence of heterogeneous precipitation on martensitic transformations in a Ni-rich NiTi shape memory alloy [J]. Materials Science and Engineering A, 2004, 378 (1−2): 148−151.
[13] ZHOU Y M, ZHANG J, FAN G L, DING X D, SUN J, REN X B, OTSUKA K. Origin of 2-stage R-phase transformation in low-temperature aged Ni-rich Ti−Ni alloys [J]. Acta Materialia, 2005, 53(20): 5365−5377.
[14] ZOU W H, HART X D, WANG R, ZHANG Z, ZHANG W Z, LAI J K L. TEM and HREM study of the interphase interface structure of Ti_3Ni_4 precipitates and parent phase in an aged TiNi shape memory alloy [J]. Materials Science and Engineering A, 1996, 219(1−2): 142−147.
[15] GALL K, JUNTUNEN K, MAIER H J, SEHITOGLU H, CHUMLYAKOV Y I. Instrumented micro-indentation of NiTi shape memory alloys [J]. Acta Materialia, 2001, 49(16): 3205−3217.
[16] GALL K, MAIER H J. Cyclic deformation mechanisms in precipitated NiTi shape memory alloys [J]. Acta Materialia, 2002, 50(18): 4643−4657.
[17] KHALIL-ALLAFI J, DLOUHY A, EGGELER G. Ni_4Ti_3-precipitation during aging of NiTi shape memory alloys and its influence on martensitic phase transformations [J]. Acta Materialia, 2002, 50(17): 4255−4274.
[18] FAN G L, CHEN W, YANG S, ZHU J H, REN X B, OTSUKA K. Origin of abnormal multi-stage martensitic transformation behavior in aged Ni-rich Ti−Ni shape memory alloys [J]. Acta Materialia, 2004, 52(14): 4351−4362.
[19] FAN G, ZHOU Y, CHEN W, YANG S, REN X, OTSUKA K. Precipitation kinetics of Ni_4Ti_3 in polycrystalline Ni-rich TiNi alloys and its relation to abnormal multi-stage transformation behavior [J]. Materials Science and Engineering A, 2006, 438−440: 622−626.
[20] DLOUHÝ A, BOJDA O, SOMSEN C, EGGELER G. Conventional and in-situ transmission electron microscopy investigations into multistage martensitic transformations in Ni-rich NiTi shape memory alloys [J]. Materials Science and Engineering A, 2008, 481−482: 409−413.
[21] KIM J I, MIYAZAKI S. Effect of nano-scaled precipitates on shape memory behavior of Ti-50.9at.%Ni alloy [J]. Acta Materialia, 2005, 53(17): 4545−4554.
[22] SHAKERI M S, KHALIL-ALLAFI J, ABBASI-CHIANEH V, GHABCHI A. The influence of Ni_4Ti_3 precipitates orientation on two-way shape memory effect in a Ni-rich NiTi alloy [J]. Journal of Alloys and Compounds 2009, 485 (1−2): 320−323.

固溶处理及时效对镍钛形状记忆合金组织演化及力学性能的影响

江树勇[1]，赵亚楠[1]，张艳秋[1]，胡 励[2]，梁玉龙[2]

1. 哈尔滨工程大学 工程训练中心，哈尔滨 150001；
2. 哈尔滨工程大学 材料科学与化学工程学院，哈尔滨 150001

摘 要：将镍钛形状记忆合金 $Ni_{50.9}Ti_{49.1}$ (摩尔分数)在 1123 K 固溶处理 2 h，然后分别在 573、723 和 873 K 时效 2 h。采用透射电镜、高分辨率透射电镜、扫描电镜和压缩实验，系统研究固溶处理和时效对镍钛合金组织演化及力学性能的影响。结果表明：固溶处理有助于消除原始镍钛样品中的 Ti_2Ni 相，但不能消除 TiC 相。固溶处理导致镍钛合金中原子排列的有序畴界。在所有时效镍钛样品中，Ni_4Ti_3 析出相、*R* 相和 *B*2 奥氏体相共存于室温下的镍钛基体上，然而在 873 K 时效的镍钛样品中，可以观察到马氏体孪晶。在 573 和 723 K 时效的镍钛样品中，细小密集的 Ni_4Ti_3 相均匀分布在镍钛基体上，而且与 *B*2 基体保持共格关系。然而，在 873 K 时效的镍钛样品中，Ni_4Ti_3 相尺寸非常不均匀，和 *B*2 基体保持共格、半共格和非共格关系。在 723 K 时效的条件下，细小均匀的 Ni_4Ti_3 相阻碍位错运动，导致最大的位错滑移临界分切应力，因此镍钛样品表现出最高的屈服强度。

关键词：镍钛合金；形状记忆合金；组织演化；力学性能；固溶处理；时效

(Edited by Chao WANG)